



FE258822

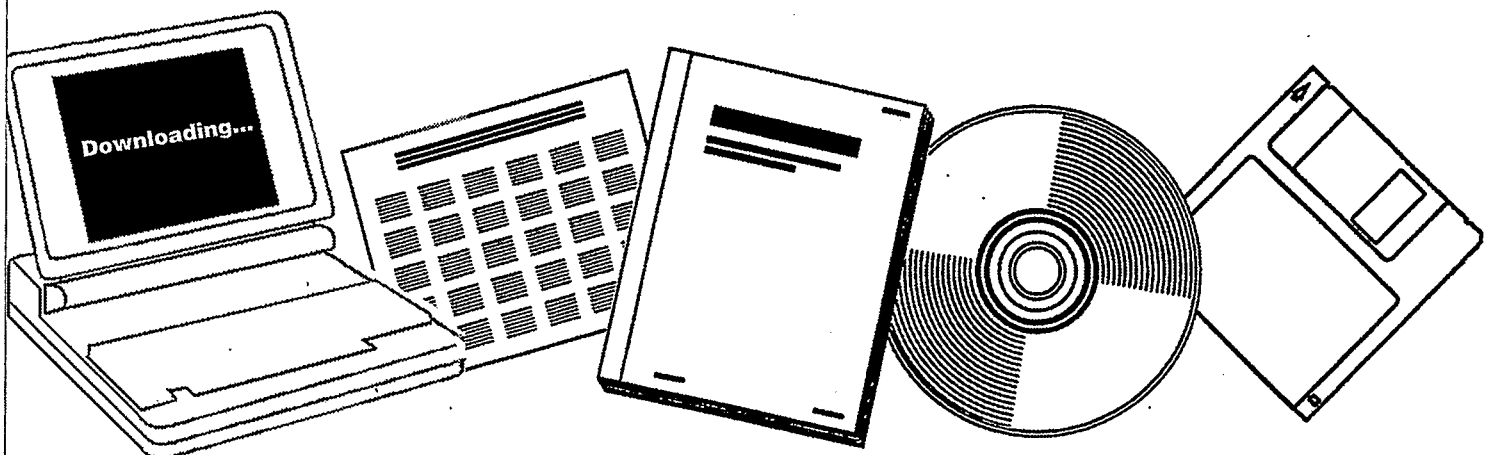
NTIS

One Source. One Search. One Solution.

**STUDY OF EBULLATED BED FLUID DYNAMICS FOR
H-COAL. QUARTERLY PROGRESS REPORT NO. 6,
MARCH 1-MAY 31, 1979**

**AMOCO OIL CO., NAPERVILLE, IL. RESEARCH
AND DEVELOPMENT DEPT**

JUN 1979



U.S. Department of Commerce
National Technical Information Service

One Source. One Search. One Solution.

NTIS



Providing Permanent, Easy Access to U.S. Government Information

National Technical Information Service is the nation's largest repository and disseminator of government-initiated scientific, technical, engineering, and related business information. The NTIS collection includes almost 3,000,000 information products in a variety of formats: electronic download, online access, CD-ROM, magnetic tape, diskette, multimedia, microfiche and paper.



Search the NTIS Database from 1990 forward

NTIS has upgraded its bibliographic database system and has made all entries since 1990 searchable on www.ntis.gov. You now have access to information on more than 600,000 government research information products from this web site.

Link to Full Text Documents at Government Web Sites

Because many Government agencies have their most recent reports available on their own web site, we have added links directly to these reports. When available, you will see a link on the right side of the bibliographic screen.

Download Publications (1997 - Present)

NTIS can now provides the full text of reports as downloadable PDF files. This means that when an agency stops maintaining a report on the web, NTIS will offer a downloadable version. There is a nominal fee for each download for most publications.

For more information visit our website:

www.ntis.gov



U.S. DEPARTMENT OF COMMERCE
Technology Administration
National Technical Information Service
Springfield, VA 22161

FE258822



FE-2588-22

Distribution Category UC-90d

STUDY OF EBULLATED BED FLUID DYNAMICS FOR H-GOAL

QUARTERLY PROGRESS REPORT NO. 6
MARCH 1-MAY 31, 1979

I. A. VASALOS, E. M. BILD, D. N. RUNDELL, J. W. GORMAN

DATE PUBLISHED: JUNE, 1979

CONTRACT EF-77-G-01-2588

Research and Development Department
Amoco Oil Company
P. O. Box 400
Naperville, Illinois
60540

TABLE OF CONTENTS

	<u>Page</u>
FOREWORD	6
OBJECTIVES AND SCOPE OF WORK	7
SUMMARY OF PROGRESS TO DATE	7
Unit Modifications	7
Data Collection	7
Model Development	9
CONSTRUCTION OF GOLD FLOW UNIT AND DATA COLLECTION	9
Unit Modifications	9
Data Collection	10
Coal Char Characterization	10
Viscosity and Surface Tension Measurement	10
Bubble Size Determination	10
Catalyst Bed Settling Rate	11
Coal Fine Settling Rate	12
Unit Data	12
MODEL DEVELOPMENT	19
FUTURE PLANS	20
NOMENCLATURE	21
TABLE I	22
CUMULATIVE SIZE DISTRIBUTION OF COAL CHAR FROM HRI	
TABLE II	23
CUMULATIVE SIZE DISTRIBUTION OF COAL CHAR NOW IN USE	
TABLE III	24
TERMINAL BUBBLE VELOCITY	
TABLE IV	25
CONDITIONS FOR CATALYST BED SETTLING RATE TESTS, HDS-2A, $l/d = 3$, CATALYST	
TABLE V	26
FINES SETTLING RATE	
TABLE VI	27
EXPERIMENTAL TESTS COMPLETED	
TABLE VII	31
CALCULATED HOLDUPS, RUN 300	
TABLE VIII	32
% BED EXPANSION FOR RUN 301: KEROSENE	
TABLE IX	33
% BED EXPANSION FOR RUN 212	
TABLE X	34
% BED EXPANSION FOR RUN 213	
TABLE XI	35
% BED EXPANSION FOR RUN 214	
TABLE XII	36
CALCULATED HOLDUPS, RUN 301: DENSE PHASE	
TABLE XIII	37
CALCULATED HOLDUPS, RUN 212: DENSE PHASE	
TABLE XIV	38
CALCULATED HOLDUPS, RUN 213: DENSE PHASE	
TABLE XV	39
CALCULATED HOLDUPS, RUN 214: DENSE PHASE	
TABLE XVI	40
CALCULATED HOLDUPS, RUN 301: DILUTE PHASE	
TABLE XVII	41
CALCULATED HOLDUPS, RUN 212: DILUTE PHASE	
TABLE XVIII	42
CALCULATED HOLDUPS, RUN 213: DILUTE PHASE	

		<u>Page</u>
TABLE XIX	BHATIA-EPSTEIN MODEL RESULTS: RUN 212-- KEROSENE/0% FINES/NITROGEN	43
TABLE XX	BHATIA-EPSTEIN MODEL RESULTS: RUN 213-- KEROSENE/0% FINES/HELIUM	44
TABLE XXI	BHATIA-EPSTEIN MODEL RESULTS: RUN 100-- WATER/0% FINES/NITROGEN	45
TABLE XXII	BHATIA-EPSTEIN MODEL RESULTS: RUN 206-- 58-74 (RUN 211) KEROSENE/16.5 VOL% FINES/ NITROGEN	46
TABLE XXIII	CONDITIONS OF TRACER TEST PERFORMED 4/6/79-- KEROSENE, NITROGEN, 70°F	47
TABLE XXIV	CONDITIONS OF TRACER TESTS PERFORMED 4/20/79-- KEROSENE, NITROGEN, HDS-2A 1 = 3/16" CATALYST, 70°F	48
TABLE XXV	CONDITIONS OF TRACER TEST PERFORMED 5/15/79-- KEROSENE/15 VOL% COAL CHAR/NITROGEN/HDS-2A 1/d = 3, 70°F	49
Figure 1	CALIBRATION OF INTEGRAL ORIFICE METER WITH HELIUM	50
Figure 2	CATALYST BED SETTLING RATE, NITROGEN, RUN 212	51
Figure 3	CATALYST BED SETTLING RATE, NITROGEN, RUN 212	52
Figure 4	CATALYST BED SETTLING RATE, NITROGEN, RUN 212	53
Figure 5	CATALYST BED SETTLING RATE, HELIUM, RUN 213	54
Figure 6	CATALYST BED SETTLING RATE, HELIUM, RUN 213	55
Figure 7	CATALYST BED SETTLING RATE, HELIUM, RUN 213	56
Figure 8	CATALYST BED SETTLING RATE, NITROGEN, 15 VOL% COAL CHAR, KEROSENE	57
Figure 9	CATALYST BED SETTLING RATE, NITROGEN, 15 VOL% COAL CHAR, KEROSENE	58
Figure 10	CATALYST BED SETTLING RATE, NITROGEN, 15 VOL% COAL CHAR, KEROSENE	59
Figure 11	DRIFT FLUX VS. GAS HOLDUP--RUN 300: KEROSENE/ NITROGEN	60
Figure 12	% BED EXPANSION VS. U_g --RUN 301: KEROSENE/0% FINES/CATALYST 1/d = 6	61
Figure 13	% BED EXPANSION VS. U_g --RUNS 212 AND 213: KEROSENE/0% FINES	62
Figure 14	CATALYST HOLDUP VS. U_g --RUN 301: KEROSENE/0% FINES	63
Figure 15	CATALYST HOLDUP VS. U_g --RUNS 212 AND 213: KEROSENE/0% FINES	64
Figure 16	BED VOIDAGE VS. SUPERFICIAL LIQUID VELOCITY: RUN 301	65
Figure 17	BED VOIDAGE VS. SUPERFICIAL LIQUID VELOCITY: KEROSENE/0% FINES	66
Figure 18	BED VOIDAGE VS. SUPERFICIAL LIQUID VELOCITY: RUN 214--KEROSENE/15 VOL% FINES/150°F	67
Figure 19	DRIFT FLUX VS. GAS HOLDUP, RUN 301: KEROSENE/ 0% FINES	68
Figure 20	DRIFT FLUX VS. GAS HOLDUP, RUNS 212 AND 213: KEROSENE/0% FINES	69

Page

Figure 21	SOLUTION OF THE BHATIA-EPSTEIN MODEL	70
Figure 22	EFFECT OF n ON THE BHATIA-EPSTEIN CORRELATION	71
Figure 23	SENSITIVITY OF THE BHATIA-EPSTEIN MODEL TO X_k	72
Figure 24	SENSITIVITY OF THE BHATIA EPSTEIN MODEL TO U_{t_e}	73
Figure 25	COMPARISON OF EXPERIMENTAL AND BHATIA-EPSTEIN MODEL CATALYST HOLDUPS: RUN 212--KEROSENE/0% FINES	74
Figure 26	COMPARISON OF EXPERIMENTAL AND BHATIA-EPSTEIN MODEL GAS HOLDUPS: RUN 212--KEROSENE/0% FINES	75
Figure 27	COMPARISON OF EXPERIMENTAL AND BHATIA-EPSTEIN MODEL HOLDUPS: RUN 213--KEROSENE/0% FINES	76
Figure 28	METHODOLOGY OF SOLUTION	77
Figure 29	SCHEMATIC DIAGRAM OF MODEL SYSTEM	78
Figure 30	EXAMPLE OF CATALYST DISTRIBUTION AT THE TOP OF THE CATALYST BED	79
Figure 31	DATA COLLECTION--FUTURE PLANS	80
APPENDIX	GAS RADIOACTIVE TRACER TESTS	81

FOREWORD

The H-Coal process, developed by Hydrocarbon Research, Incorporated (HRI), involves the direct catalytic hydroliquefaction of coal to low-sulfur boiler fuel or synthetic crude oil. The 200-600 ton-per-day H-Coal pilot plant is being constructed next to the Ashland Oil, Incorporated refinery at Catlettsburg, Kentucky under ERDA contract to Ashland Synthetic Fuels, Incorporated. The H-Coal ebullated bed reactor contains at least four discrete components: gas, liquid, catalyst, and unconverted coal and ash. Because of the complexity created by these four components, it is desirable to understand the fluid dynamics of the system. The objective of this program is to establish the dependence of the ebullated bed fluid dynamics on process parameters. This will permit improved control of the ebullated bed reactor.

The work to be performed is divided into three parts: review of prior work, cold flow model construction and operation, and mathematical modeling. The review of prior work has been completed. The objective of this quarterly progress report is to outline progress in the second and third parts during the seventh quarter of the project.

OBJECTIVES AND SCOPE OF WORK

The overall objective of this project is to improve the control of the H-Coal reactor through a better understanding of the hydrodynamics of ebullated beds. The project is divided into three main tasks:

- 1) Review of prior work in three-phase fluidization.
- 2) Construction of a cold flow unit and collection of data.
- 3) Development of a mathematical model to describe the behavior of gas/liquid fluidized beds. The model will be based on information available in the literature and on data generated in the cold flow unit.

Progress in Part 1 has already been reported in previous reports. Progress made in Parts 2 and 3 during this quarter is presented in this quarterly status report.

SUMMARY OF PROGRESS TO DATE

Unit Modification

A Tuthill rotary pump was installed on the unit. It was piped into the system so that it can be used either as the feed or recycle pump. The pump can be used to attain higher liquid flow rates and can handle larger quantities of gas than the pumps previously in use. The Tuthill pump has worked well without any major problems for several months.

The orifice size in the integral orifice meter was changed and calibrated for testing with helium.

Data Collection

Continued characterization of coal char and gas/liquid systems. Several more barrels of coal char will be required for testing, and samples from HRI were screened to find barrels that match the particle size now in use.

Due to continuing problems in measuring slurry viscosity with the capillary tube viscometer, samples were sent to Rotary Drilling Services, who use a Fann VG meter to measure slurry viscosity. They measured the viscosity of a 15 vol% coal char/kerosene slurry at 72, 100, and 150°F, giving results of 5, 5, and 4 cp, respectively.

Core Laboratories can measure the surface tension of kerosene saturated with the gases used in the fluid dynamics unit over a range of pressures. Samples will be sent to them next quarter.

Gas bubble sizes at the reactor walls were determined at different flow conditions and locations in the reactor using photographs. Gas bubbles average about 0.35 mm in diameter.

Both catalyst bed and coal fines settling rates were determined this quarter. The level of catalyst in one case and fines in the other were monitored with a gamma-ray scanner following the sudden loss of both gas and liquid flow. Liquid flow rate and gas type have significant effects on the catalyst bed settling rate. Fines settling is very slow and requires overnight determinations. These tests will be completed next quarter.

Completed replicate experiments with nitrogen, kerosene, and HDS-2A catalyst (3/16" length) with 0 vol% and 15 vol% coal char. Experiments with the 15 vol% slurry were conducted at 150°F. Tests using helium or nitrogen with kerosene and the standard catalyst were also completed. The HDS-2A catalyst with $l/d = 6$ was also tried with kerosene and nitrogen, but broke up too much for extensive testing. Bed expansions and catalyst holdups were determined from bed heights measured with the gamma-ray scanner. Liquid holdups were determined by gamma-ray scans and DP measurements. Fines distribution along the reactor was found by sampling.

Data obtained over a range of operating conditions were correlated with models identified in the literature. Liquid/catalyst data were correlated using the Richardson-Zaki equation, which relates the liquid holdup to the nth power to the ratio of liquid superficial velocity to the catalyst terminal velocity. The index, n, was determined for all tests and compared with previous results.

Gas/liquid/catalyst data were analyzed using two different correlations: the drift flux model of Darton and Harrison, and the generalized wake model of Bhatia and Epstein. It was found that the drift flux model is useful in defining flow regimes and unstable bed operation, but since most of our data lie in the transition region, it cannot be used as a quantitative tool to calculate holdups.

Initial tests of the Bhatia-Epstein model with our data are very promising. However, the model is most sensitive to input values of terminal bubble velocity, which is not easily determined.

Completed several tracer tests at a variety of conditions. The data were analyzed and first and second moments of the concentration-time curves calculated. Complex mixing phenomena are taking place, and through visual observation and discussions with Professor Aris it is apparent that there is considerable gas backmixing in the reactor. He

is currently developing a model including both gas upflow and downflow which will be tested with our data.

Model Development

A running version of the raw data analysis subprogram of the master computer program was completed. Two additional modeling subroutines were added to the program. One subroutine calculates the drift flux for the Darton-Harrison correlation. The other subroutine calculates the catalyst distribution at the top of the catalyst bed using an error function.

In addition, an independent computer program was written for the iterative solution of the Bhatia-Epstein model. A version of the Complex optimization routine modified to interact with the Bhatia-Epstein correlation is being added to the master program.

CONSTRUCTION OF COLD FLOW UNIT AND DATA COLLECTION

Unit Modifications

The Tuthill rotary pump was installed in the unit this quarter. The pump was piped in parallel to both the existing feed and recycle pumps so that it can be used to replace either pump. Pumping capacity is controlled via a Reeves motordrive, eliminating the problem of fines' plugging a control valve. Reactor liquid velocities of up to 135 gpm/ft² were achieved with the new pump.

The Tuthill pump will run dry without damage, so it can be used on the recycle line, even when large quantities of gas are entrained in the line. The pump has worked well without any major problems for several months.

Channeling of gas and liquid through the catalyst bed was noted. Shortly after this observation, most of the catalyst backflowed out of the reactor. The bubble cap had become detached from the distributor section, resulting in these problems. The nut holding the bubble cap had apparently worked itself loose during testing; a lock washer has now been added to the assembly.

As a result of the catalyst backflow from the reactor, the feed line became plugged with catalyst. To prevent future backflow of catalyst out of the reactor, a swing check valve was ordered. It will be installed in the feed line the next time the system is down.

The orifice in the integral orifice meter was changed for testing with helium so that the same range of superficial velocities is used with both nitrogen and helium. The calibration of the integral orifice meter with helium is shown in Figure 1.

Data Collection

Coal Char Characterization.--Coal char, in addition to the eight barrels already received from HRI, will be needed for future testing. Particle size analysis of samples from 15 additional barrels at HRI was completed. The results are given in Table I. The particle size distribution to be matched is shown in Table II. The size analysis was performed at IIT Research Institute using an optical microscope interfaced with the Quantimet 720 computerized image analyzer. Very few of the new samples closely match the particle size distribution of coal char currently in use. Six barrels were chosen out of the set for shipment to Amoco, as annotated in Table I.

Viscosity and Surface Tension Measurement.--Due to continuing problems with plugging in the capillary tube viscometer as described in Quarterly Progress Report No. 5 (March, 1979), other methods to measure slurry viscosity were investigated. Rotary Drilling Services in Tulsa, Oklahoma, use a Fann VG Model 50 meter to measure viscosity. The meter consists of a rotating sleeve and a spring-loaded bob giving a direct reading of the viscosity. They measured the viscosity of a 15 vol% coal char/kerosene slurry at 72, 100 and 150°F, giving results of 5, 5, and 4 cp, respectively. These are slightly higher than values determined with the capillary tube viscometer; however, the results are probably more reliable because of the problems with fines settling in the capillary tube viscometer. Samples of 5, 10, and 16.5 vol% coal char slurries will be sent for viscosity measurement.

Previous tests with helium and Freon-12 used as the fluidizing gas instead of nitrogen indicate the gas has greater effect on the system fluid dynamics than can be explained by density effects alone. This is especially true in the case of Freon-12, which absorbs significantly in kerosene. The effect of these gases on surface tension will be measured by Core Labs. The pendant drop method will be used to measure the surface tension between a liquid and a gas. The device consists of a windowed, high pressure and temperature cell containing a dropper tip. The cell is filled with the gas and the liquid is introduced through the dropper tip to form a pendant drop. As the system equilibrates, photographs are made of the drop. The cost for the testing will be \$500 per liquid/gas system. These measurements will be completed next quarter.

Bubble Size Determination.--In order to determine gas bubble sizes in the reactor at different flow conditions, photographs were taken of the unit fluidized with kerosene and N₂. Only bubbles close to the reactor wall could be measured. Pictures were taken at three different flow conditions and at one location just above the catalyst bed and at another

just below the recycle cup. In all cases the liquid velocity was 0.1 ft/sec and gas velocity was either 0.05, 0.1, or 0.2 ft/sec.

All pictures are very similar, and the only difference visually is the existence of a few larger bubbles at $U_g = 0.2$ ft/sec at both reactor locations. Bubble size varied from 0.2 mm to 1.6 mm in diameter; most bubbles were about 0.35 mm in diameter. The smaller bubbles were all spherical in shape; however, some of the largest bubbles were beginning to become elliptical.

Using the Peebles and Garber correlations, the terminal bubble velocity was calculated for the three bubble sizes, 0.2, 0.35, and 1.6 mm in diameter. These are given in Table III.

Catalyst Bed Settling Rate.--Tests evaluating catalyst settling rate following a sudden loss of both gas and liquid flow were performed this quarter. The conditions for each test are given in Table IV. Bed heights were determined using the gamma-ray scanner.

Plots of bed height versus time for catalyst beds fluidized with kerosene and nitrogen are shown in Figures 2, 3, and 4. It required about eight seconds for the catalyst bed to completely collapse with a liquid velocity of 0.10 ft/sec. The flow rate of N_2 did not appear to have a significant effect on settling time. At the higher liquid flow of 0.20 ft/sec, the settling time increased to 17 seconds.

Plots of bed height versus time for beds fluidized with kerosene and helium are shown in Figures 5, 6, and 7. These results also indicate gas flow rate does not affect settling time, but an increase in liquid flow increases the time required for the catalyst bed to settle. However, significantly longer times were required for complete settling of catalyst beds fluidized with helium instead of N_2 . At a liquid flow rate of 0.10 ft/sec, the bed required over 12 seconds to settle compared with the 8 seconds for beds fluidized with N_2 . This trend is difficult to explain because it is the reverse of what is expected. Helium, as will be discussed later, tends to form larger bubbles than nitrogen. The larger, less dense bubbles should leave the bed more quickly than the smaller N_2 bubbles. This result may be related to the effect helium has on kerosene fluid properties and, as mentioned previously, is under investigation.

Plots of bed height versus time for beds fluidized with 15 vol% coal char/kerosene slurry and nitrogen are given in Figures 8, 9, and 10. Again, superficial liquid velocity has a much greater effect on settling time than superficial gas velocity. At a liquid velocity of 0.10 ft/sec, and gas velocities of 0.10 and 0.15 ft/sec, the settling times were 19 and 22 seconds, respectively. However, when the superficial liquid velocity was increased to 0.15 ft/sec, the settling time increased to about 35 sec. As expected, settling times with the kerosene slurry were significantly longer than with kerosene and either nitrogen or helium due to the higher fluid viscosity.

Coal Fine Settling Rate.--Tests to determine the coal fine settling rate were started this quarter. Coal fine settling is very slow in kerosene, so these tests were run overnight. Coal fine concentration at several points along the reactor was monitored with the gamma-ray scanner. The results from two tests are shown in Table V. Data were collected using 50 and 55" increment scan positions. At the 50 and 55" levels, the count rate dropped significantly just over an hour after flow to the reactor was stopped. This indicates that the fines collecting on top of the catalyst bed had reached that level. At higher locations in the reactor, the count rate increases as the fines settle. At 165", the fines had all settled between 6-8 hours and at 150", the count rate increased after 6 hours. The coal fines had dropped below the 100" level after ten hours. Further scans at several other locations in the reactor will be completed next quarter.

Unit Data.--Kerosene with 0 or 15 vol% coal char was used to fluidize the catalyst bed for all tests performed this quarter. Either N₂ or He was used as the fluidizing gas. Experiments were also conducted with two different catalysts, HDS-2A with l/d = 3 and 6. Experimental test conditions for runs carried out this quarter are given in Table VI. A summary is shown below:

Run No.	Temp, °F	Fines, Vol%	Test Nos.	Gas	l/d	Liquid Flow Rate Range, GPM/Ft ²	Gas Flow Rate Range, Ft/Sec
300	72	0.0	01-20	N ₂	None	22.4-89.7	0.05-0.25
301	72	0.0	01-16	N ₂	6	37.6-119.0	0-0.16
212	72	0.0	01-15	N ₂	3	30.8-88.7	0-0.23
213	72	0.0	01-22	He	3	36.7-109.5	0-0.25
214	150	15.0	01-13		3	38.0-75.6	0.0

Experimental results for gas/liquid tests, Run 300, are given in Table VII.. The liquid holdups were calculated using both gamma-ray and DP data. In general, there is good agreement between the calculated values of the two methods.

To correlate the gas/liquid data, the two-phase gas drift flux was calculated:

$$V_{CD} = U_g(1 - \epsilon_g) - U_1\epsilon_g$$

Calculated values of drift flux are also given in Table VII. A plot of drift flux vs. gas holdup is shown in Figure 11. Models to predict gas drift flux developed by Richardson and Zaki and Davidson and Harrison are also shown on the plot. Data at U₁ = 22.4 gpm/ft² fall along the Davidson-Harrison line; data collected at all other velocities are modelled most closely by the Richardson-Zaki correlation.

The Davidson-Harrison (1) approach assumes that the cloud of bubbles rises at the same velocity as a single bubble, similar to plug flow. The Richardson-Zaki equation applies to bubbles which behave as solid particles of zero density. Small bubbles are more likely to behave like solid particles. Interface impurities also tend to cause the bubbles to behave as solid particles.

These results imply that at low liquid flow rate the bubbles rise in plug flow. However, at higher liquid velocities there may be interaction between the bubbles affecting the rise velocity of the cloud.

Catalyst bed heights for the remaining runs were determined using the gamma-ray scanner on the reactor. Bed heights and per cent bed expansion for Run 301 are given in Table VIII. During testing with this catalyst, $l/d = 6$, the particles began to break up. Significant fracturing of the catalyst started during Test 301-07.

Due to the continual change in catalyst particle size distribution, initial bed height and bed expansion changed at constant flow conditions. Therefore, % bed expansion was calculated with revised values of initial bed height as the catalyst broke up. The plot of % bed expansion vs. U_g with U_l as a parameter is shown in Figure 12. Before significant breakup occurred, bed expansions were much lower than those experienced with catalyst $l/d = 3$, for example, at liquid flow = 0.10 ft/sec, 11% vs. about 40%. As catalyst broke up, bed expansions increased. When the test at $U_l = 0.15$ ft/sec, $U_g = 0.15$ ft/sec was run, the bed expansion of about 78% was nearly the same as with the catalyst with $l/d = 3$ (76%).

Bed expansion of the unbroken catalyst particles is lower due to the increased gravitational force. Buoyant and drag forces on the particle also increase, but to a much lesser extent because these forces are most sensitive to changes in particle diameter.

Bed heights and per cent bed expansions for Run 212 are given in Table IX. Tests from Run 212 are replicates of the earlier series Run 201. A plot of bed expansion vs. gas velocity with liquid velocity as a parameter is shown in Figure 13. The liquid velocity, 31.4 gpm/ft², is below minimum fluidization velocity, thus explaining the negligible increase in bed expansion upon increasing the liquid flow rate. The bed is fluidized at $U_l = 38.1$ gpm/ft². As gas is added to the liquid fluidized bed, the expansion consistently increased.

Bed heights and per cent bed expansions are given in Table X for tests with kerosene, catalyst, and helium, Run 213. The plots of per cent bed expansion versus gas velocity are also shown in Figure 13. Bed expansions with helium were generally lower than the expansions with nitrogen. However, the differences are within experimental error. The only exception is at $U_l = 67$ gpm/ft²; when the helium gas velocity was increased to 0.2 ft/sec, the catalyst bed contracted significantly. No explanation of this phenomenon can be offered at this time.

Bed heights and per cent bed expansions for Run 214 are reported in Table XI. This run is a replicate of the earlier series Run 208. All of the data are at zero gas flow rate.

Catalyst holdups for all tests performed this quarter were determined from bed heights. Gamma-ray scans of the reactor and DP measurements were used to calculate liquid holdups. Calculated holdups in the catalyst bed for Runs 301, 212, 213, and 214 are reported in Tables XII, XIII, XIV, and XV, respectively. Plots of catalyst holdup versus gas velocity with liquid velocity as a parameter are shown in Figures 14 and 15 for Runs 301, 212, and 213. The same trends noted with bed expansion can also be seen with these plots. In summary, comparison of Runs 212 and 213 indicates a change in gas density has minimal effect on catalyst holdup. For Run 301, the large decrease in catalyst holdup as catalyst breakup occurred can be noted. Calculated holdups in the dilute phase for Runs 301, 212, and 213 are shown in Tables XVI, XVII, and XVIII.

Liquid catalyst data were analyzed with the Richardson-Zaki equation:

$$e_1^n = U_1/U_t$$

A plot of e_1 vs. U_1 is given in Figure 16 for Run 301. Most catalyst breakup occurred after the liquid/catalyst tests were completed. Therefore, these results should be reasonably reliable. However, high liquid velocities were not used because of the severe catalyst breakup which would occur, and the bed was not fluidized at the lower liquid velocities. Thus, the value of n was based on only three data points. The n determined from the limited data is 2.3

A plot of e_1 or $(1 - e_c)$ versus U_1 is given in Figure 17 for Run 212. Linear regression was used to determine the slope of the line which corresponds to the Richardson-Zaki index, n . This was determined to be 3.3. This value is larger than the one found previously for kerosene/HDS-2A $l/d = 3$ catalyst. However, the values are within the 10% experimental error.

The plot of e_1 vs. U_1 for Run 214 is given in Figure 18. The Richardson-Zaki index was determined to be 4.0. The value found for Run 208, 3.7, is within experimental error of these replicate tests.

Three-phase data were analyzed using two different correlations: Darton-Harrison drift flux and Bhatia-Epstein generalized wake model. Results of the drift flux analysis will be reviewed first.

Drift flux for a three-phase system is described as:

$$V_{CD} = U_g(1 - e_g) - \frac{U_1(1 - e_g)e_g}{e_1}$$

On plots of V_{CD} versus e_g , lines identifying two flow regimes are defined: churn turbulent and ideal bubbly. Calculated drift fluxes for Runs 301, 212, and 213 are given in Tables XII, XIII, and XIV. A plot

of drift flux for Run 301 is given in Figure 19. Evaluation of this plot is difficult due to the continual breakup of catalyst.

A plot of drift flux for both Runs 212 and 213 is shown in Figure 20. As found previously, the flow regime remains in ideal bubbly flow over these flow rates if the bed is fluidized with nitrogen and kerosene. However, when helium and kerosene were used to fluidize the bed at the same flow rates, the flow regime started to make the transition into churn turbulent flow. This is unexpected due to the similarity of bed expansions for both cases. The use of helium must affect the flow transition through a change in kerosene surface tension. Therefore, the surface tension of kerosene under helium pressure should be determined.

In order to further evaluate the effect of gas density on three-phase fluidization, tests should be performed with a gas which has greater density than N_2 . Previous tests with Freon-12 cannot be analyzed until the effect of the substantial absorption of Freon-12 in kerosene on fluid properties is evaluated.

Another gas which has a greater density than N_2 is SF_6 . The absorption of SF_6 in kerosene was checked and found to be 470 cc SF_6 per liter of kerosene at 15 psig. Although this is less than the absorption of Freon-12, it could still substantially change the surface properties. Therefore, evaluating the properties of kerosene saturated with Freon-12 will be pursued instead of trying further tests with SF_6 .

The Bhatia-Epstein generalized wake model was used to analyze tests performed this quarter. In addition, tests from Run 100 with water/ N_2 /catalyst and Run 206 with 16.5 vol% coal char/kerosene slurry/ N_2 /catalyst were analyzed with this model. The equations used to solve this model are shown in Figure 21.

Initially, the sensitivity of the model to changes in several parameters was examined. The effect of changes in the Richardson-Zaki index, n , on catalyst and liquid holdups is shown in Figure 22. The index can generally be determined within 10%, so error in calculated holdups would be much less than shown in Figure 22. The sensitivity of the solution to changes in the ratio of wake solids to particulate-phase solids, X_k , is shown in Figure 23. Again, small changes in X_k have little effect on the calculated holdups.

The effect of changes in the terminal bubble velocity on the calculated holdups is given in Figure 24. Of all the values input to the model, U_{t_B} is currently the hardest to define and has the largest error associated with it. Solution of the Bhatia-Epstein model is most sensitive to terminal bubble velocity.

It should also be noted that solutions for catalyst holdup are not unique, and that the same catalyst holdup can be calculated for several values of U_{t_B} , X_k , and n .

A preliminary analysis of the data from Runs 212 and 213 with the Bhatia-Epstein model was performed. The variables which must be known to solve

the set of equations are: U_1 , U_g , X_k , U_t , U_{t_b} , and n . The gas and liquid velocities are known. The Richardson-Zaki index and catalyst terminal velocity were determined experimentally. The relative wake solids content, X_k , was calculated from an empirical correlation developed by El-Temtamy and Epstein (1):

$$X_k = 1 - 0.877 \frac{V_1}{U_s}$$

The value of the terminal bubble velocity was then varied to give the best fit to experimental data.

Test conditions, the calculated X_k , and the estimated U_{t_b} which gave the best fit for Run 212 are listed in Table XIX.

Comparison of the Bhatia-Epstein results with experimentally determined catalyst and gas holdups is shown in Figures 25 and 26.

The calculated values of X_k were generally close to zero, and the terminal bubble velocities which gave the best fit are relatively small. These values of U_{t_b} correspond to bubbles with diameters generally less than 0.2 mm. Bubble photographs indicate that bubbles near the reactor wall are typically about 0.35 mm in diameter, so estimated bubble terminal velocities are probably within an order of magnitude of actual bubble velocities.

Calculated values of X_k and the U_{t_b} which gave the best fit are given in Table XX for Run 213. Comparison of the calculated and experimental holdups is shown in Figure 27. The calculated values of X_k were much larger using helium as the gas than with nitrogen.

Terminal bubble velocities which gave the best fit were also larger with helium than with nitrogen. This indicates that the use of helium results in formation of larger bubbles which will entrain more solids in their wake.

These results agree with the drift flux analysis, which indicated the use of helium instead of nitrogen enhanced the transition to churn turbulent flow. The transition results from formation of larger bubbles.

Analysis of results from Run 100 with the Bhatia-Epstein model was done in the same manner as with Runs 212 and 213. Test conditions, the value of X_k calculated by the El-Temtamy and Epstein correlation, and the estimated U_{t_b} which gave the best fit are listed in Table XXI. Calculated values of X_k were larger than for either Run 212 or 213; they average above 0.8. The terminal bubble velocities which gave the best fit are also greater than for either Run 212 or 213. This indicates that with water tests, much larger bubbles are formed with large wakes containing high concentrations of catalyst particles. This is in agreement with the Darton-Harrison analysis, which showed almost all the water data to be in the churn-turbulent or bubble coalescing flow regime.

(1) El-Temtamy, S. A., and N. Epstein, Int J Multiphase Flow, 4, 19, 1978.

Results of the analysis of Run 206 58-74 with the Bhatia-Epstein model are shown in Table XXII. Calculated values of X_k were much larger than results from Run 212 or 213, averaging above 0.8 as with the water tests. Although the terminal bubble velocities which gave the best fit were 20-30 times higher than for Run 212, they were less than the values for water tests, Run 100.

These results are also in good agreement with the Darton-Harrison model. When coal fines were added to the kerosene to make a slurry, the transition to churn turbulent from ideal bubbly flow was enhanced; thus, the larger values of X_k and U_{t_B} . However, most of the data were in the transition region and did not completely make the change to churn turbulent flow, indicating why the terminal bubble velocities are smaller than the values with water.

Two runs, 212 and 206 58-74, were also analyzed with the Bhatia-Epstein equation using a correlation to calculate U_{t_B} and then varying X_k to give the best fit. The terminal bubble velocity was calculated using an empirical correlation developed by Kim, et al (2):

$$U_{t_B} = 83.1 U_1^{0.065} U_g^{0.339} \mu^{0.025} \epsilon^{0.179}$$

Using this correlation, all calculated values of U_{t_B} were about 0.2 ft/sec. Varying X_k from 0 to 1 did not result in very good fits with the experimental data. This again indicates the model is relatively insensitive to changes in X_k and U_{t_B} is the most important parameter for reliable application of the Bhatia-Epstein model.

Tests performed during the last week of May, 1979, which were replicates of earlier tests, gave anomalous results. Bed expansions were significantly higher than determined previously. Samples taken from the unit indicate that significant catalyst breakup had been occurring with the HDS-2A catalyst $1/d = 3$. This catalyst is being removed from the unit and fresh catalyst added.

Several radioactive gas tracer tests were conducted this quarter. Argon-41, the radioactive gas, was injected into the reactor bottom at two different locations. Its progress was monitored using externally mounted NaI scintillation crystal detectors. Detector location on the unit is shown in a figure in the appendix.

Conditions for the tests conducted this quarter are shown in Tables XXIII, XXIV, and XXV. A computer program was written to plot tracer data stored on the computer. Examples of these plots are also shown in the appendix.

The first and second moments of the tracer concentration-time curves were determined. Numerical integration of the curves was performed using Simpson's Rule. The first moment corresponds to the mean residence

(2) Kim, et al., Chem Eng Sci, 32, 1299, 1977.

time, and the second moment corresponds to the variance. However, with trailing time distributions, as in this case, large errors in the second moment can occur. To minimize these errors, the moments can be determined by taking the Laplace transform of the moments and evaluating the function as s approaches zero. This effectively does curve smoothing without chopping off the tails on the distribution. Calculation of the moments using this procedure, suggested by Ostergaard and Michelsen (3), is in progress.

Using the mean residence time at each detector and the distance between detectors, the gas linear velocity, V_g , at different points in the reactor can be calculated. Using the linear velocity and gas superficial velocity, the gas holdups can be calculated:

$$\epsilon_g = \frac{U_g}{V_g}$$

Calculated moments, linear velocity, and calculated holdups are listed in a table in the appendix for all tracer tests. When available, gas holdups calculated from gamma-ray scans are also given.

Except for the first tracer test, when the detectors were collimated to one-inch diameter so that the reactor center was preferentially viewed, holdups calculated from tracer data are much greater than holdups determined by gamma-ray scans. For the remaining tests, the collimators had been opened to 2 x 4" slits in order to view an entire horizontal cross-section of the reactor while maintaining a narrow vertical view.

These results indicate that the gas linear velocity measured using gamma-ray scans is significantly greater than the velocity measured with the tracer tests. This difference could result from significant backflow of gas in the reactor. The gamma-ray scan measures a point density independent of the gas direction, whereas tracer tests give a measure of the flow direction. When using gamma-ray holdups to calculate gas linear velocity, it is assumed all the gas is travelling upward, thus resulting in the overestimate of gas linear velocity.

Due to this apparent backmixing of gas in the reactor, gas holdups cannot be directly calculated from tracer data. However, gas holdups calculated from the first tracer test, 9/28/78, were similar to those calculated by gamma-ray scans. In this case the center of the reactor was preferentially seen, thus indicating the gas flows upward in the center of the reactor and the downflow of gas occurs mainly at the reactor walls.

This theory of gas upflow in the center of the reactor and gas downflow at the walls is supported by visual observations of the reactor with catalyst fluidized by kerosene and nitrogen. Large sections of gas bubbles flowing downward can be observed.

(3) Ostergaard, K., and M. L. Michelsen, Can. J of Chem Eng, 47, April, 1969.

To test this theory, a model is being developed to describe the tracer results. This model is being formulated through discussions with Professor Aris of the University of Minnesota. The basis of the model which will be tested is shown in Figure 28. This is the simplest model to describe both upflow and downflow, treating the reactor as two different sections: the catalyst bed and the dilute phase. Using this model, ten parameters will be used to describe the reactor flow system.

A simplified version of this model can be applied to results from the first tracer test. Development of this model is shown in Figure 29. Using a plot of $1/H_p q(s)$ versus s , the residence time of the upflow system can be determined. Derivation of the other parameters using the rest of the tracer tests with views of the entire reactor will be considerably more complicated. Parameter estimation of a high-order polynomial will be required. Application of both versions of the model to the experimental data will be completed next quarter.

MODEL DEVELOPMENT

Programming of a master computer program for data analysis and modeling was continued this quarter. A figure showing the basic outline for development of this program was given in Quarterly Progress Report No. 5. This quarter, a running version of the raw data analysis subprograms was completed.

Several subroutines for modeling were added to the program. One subroutine calculates drift flux for the Darton-Harrison correlation. The other subroutine is used to calculate the catalyst distribution at the top of the catalyst bed. At higher gas and liquid flow rates, the top of the catalyst bed is not always clearly defined. The holdups of the catalyst slowly drops with increasing height in the bed.

To account for this distribution, a computer program based on a correlation by Begovich and Watson (4) was developed. The expression for variation in catalyst holdup is given below:

$$\epsilon_{ch} = [(\rho_c + 1)/2]\epsilon_c$$

$$\rho_c = \text{erf}[(h - I_c)/\zeta_c]$$

The inflection point, I_c , on a holdup versus height diagram corresponds to the nominal bed height, and ζ_c corresponds to the width of the catalyst transition region. These two values are illustrated on a gamma-ray plot shown in Figure 30.

This plot shows an extreme case of catalyst distribution. For most cases, ζ_c is between 0 and 5", whereas in this case it is in excess of 30". In general, greater fluid viscosity results in a wider transition region.

(4) Begovich, J. M., and J. S. Watson, Fluidization, Cambridge University Press (1978).

In addition, a computer program was written and stored on an in-house computer for the iterative solution of the Bhatia-Epstein model. Equations used for this model and the methodology for the solution are given in Figure 21. Results of trial solutions with the model were discussed in the preceding section.

This solution of the Bhatia-Epstein model is currently being added to the master computer program, along with an optimization routine to determine optimum values for parameters in the model--i.e., U_{t_0} and X_k .

The optimization program uses a modified complex algorithm to locate optimal points of functions, subject to implicit and explicit constraints. A special coding minimizes problems with the program hanging upon a non-universal optimum (saddle point). In order to easily implement the optimization routine, a method was needed to enter constraints and variables into the system. To accomplish this, a subroutine was written to allow individual program vectors to be entered without requiring cumbersome amounts of input.

FUTURE PLANS

- 1) Complete tests with He/15 vol% coal char slurry/HDS-2A catalyst $l/d = 3$.
- 2) Clean unit and add high density equilibrium catalyst from HRI and start N_2 /kerosene/catalyst tests.
- 3) Complete addition of Bhatia-Epstein model to master computer program.
- 4) Modify computer program into a predictive model.

Plans for unit operation are shown in Figure 31.

NOMENCLATURE

d	Particle diameter.
d_p	Diameter of a circle of the same area as the projected particle in its most stable position.
d_s	Diameter of a sphere with the same volume as the particle.
D	Bed diameter.
ϵ_{cb}	Catalyst volume fraction from bed height data.
$\epsilon_{c\gamma}$	Catalyst volume fraction from gamma-ray data.
ϵ_g	Gas volume fraction.
$\epsilon_{g\gamma B}$	Gas volume fraction from bed height and γ -ray data.
ϵ_l	Liquid volume fraction.
$\epsilon_{l\gamma B}$	Liquid volume fraction from bed height and γ -ray data.
h	Height in reactor.
I_c	Inflection point on catalyst holdup curve.
n	Richardson-Zaki index.
σ	Surface tension.
δ_c	Width of catalyst transition region.
μ	Viscosity.
U_g	Superficial gas velocity.
U_l	Superficial liquid velocity.
U_s	Gas-liquid slip velocity, $\frac{U_g}{\epsilon_g} - \frac{U_l}{\epsilon_l}$
U_t	Terminal catalyst velocity.
U_{tB}	Terminal bubble velocity.
V_{cd}	Gas drift flux.
V_g	Linear gas velocity.
V_l	Linear liquid velocity.
X_k	Ratio of solids in wake to solids in particulate phase.

TABLE I

CUMULATIVE SIZE DISTRIBUTION OF COAL CHAR FROM HRI
CUMULATIVE NUMBER PERCENT GREATER THAN STATED SIZE

SAMPLE NO.	SIZE (μm)										AVG SIZE (μm)		
	0	1.1	2.7	3.8	5.4	8.1	13.5	18.9	29.7	51.3		70.2	91.8
LO-1449-1	100	83.9	60.6	49.2	38.8	28.3	18.2	11.7	6.3	2.4	0.8	0.6	4.0
* LO-1449-2	100	83.1	60.6	48.2	36.7	26.1	14.2	9.0	4.4	1.6	0.7	0.3	3.7
LO-1449-3	100	90.8	70.8	60.0	46.9	32.9	18.7	11.3	4.6	1.1	0.4	0.3	5.0
* LO-1449-4	100	83.0	54.6	42.8	31.3	20.5	10.2	6.3	3.3	0.8	0.3	0.2	3.2
* LO-1449-5	100	80.1	50.4	38.9	28.6	19.1	12.5	7.7	4.1	1.5	0.9	0.4	3.2
LO-1449-6	100	82.2	53.6	39.9	29.7	19.0	9.6	6.1	3.4	1.2	0.7	0.3	3.0
LO-1449-7	100	78.2	50.8	38.5	26.3	16.4	8.3	4.7	2.0	0.8	0.4	0.3	2.8
* LO-1449-8	100	83.5	60.2	46.0	33.5	23.0	11.7	7.7	4.0	1.6	0.7	0.2	3.5
LO-1449-9	100	80.7	49.8	37.0	26.7	16.8	8.5	5.3	2.0	0.5	0.2	0.1	2.7
LO-1449-10	100	78.8	48.7	37.6	28.1	19.3	12.3	8.5	4.6	1.3	0.4	0.3	2.9
LO-1449-11	100	78.5	47.2	33.6	22.7	13.3	6.8	4.2	2.1	0.8	0.4	0.3	2.7
LO-1449-12	100	84.7	65.6	55.5	42.7	29.6	16.0	9.9	5.2	2.0	1.1	0.6	4.0
* LO-1449-13	100	81.3	52.9	40.4	29.6	19.9	11.8	7.9	3.6	0.8	0.4	0.2	3.2
* LO-1449-14	100	83.6	56.0	43.0	31.7	21.1	11.4	7.9	3.6	1.2	0.6	0.2	3.6
LO-1449-15	100	90.1	69.2	56.5	43.6	29.9	17.0	11.3	5.1	1.6	0.8	0.4	4.7

*Barrels selected.

TABLE II

CUMULATIVE SIZE DISTRIBUTION OF COAL CHAR NOW IN USECUMULATIVE NUMBER AND NUMBER %
GREATER THAN STATED SIZE

<u>Size, μm</u>	<u>Cumulative Number</u>	<u>Cumulative Number %</u>
0	2916	100
1.1	2635	90.4
2.7	1921	65.9
3.8	1396	47.9
5.4	922	31.6
8.1	529	18.1
13.5	212	7.3
18.7	115	3.9
29.7	64	2.2
51.3	24	0.8
72.8	13	0.4
94.4	8	0.3

TABLE III
TERMINAL BUBBLE VELOCITY

Bubble Diameter, mm	0.2	0.35	1.6
Terminal Bubble Velocity, Ft/Sec	0.04	0.09	0.65

EMB/ml
5/16/79

TABLE IV
 CONDITIONS FOR CATALYST BED SETTLING
RATE TESTS, HDS-2A CATALYST $1/d = 3$

<u>Slurry</u>	<u>Gas</u>	<u>U₁</u> <u>Ft/Sec</u>	<u>U_g</u> <u>Ft/Sec</u>
Kerosene/0% Fines	N ₂	0.10	0.10
" "	"	0.10	0.15
" "	"	0.20	0.10
" "	He	0.10	0.10
" "	"	0.10	0.15
" "	"	0.20	0.10
Kerosene/15 Vol% Fines	N ₂	0.10	0.10
" "	"	0.10	0.15
" "	"	0.15	0.10

EMB/ml
 6/21/79

TABLE V

FINES SETTLING RATE:
GAMMA RAY SCANS (CPS)

Reactor Position (In.)	<u>0</u>	<u>2</u>	<u>4</u>	<u>6</u>	<u>8</u>	<u>10</u>	<u>12</u>	<u>14</u>	<u>16</u>
50	273.5	232	225	225	231	235	234	238	26
100	275.4	276	278	285	279	298	303	298	295
150	261	277	275	281	284	285	290	283	282
Min.	0	20	40	60	80	100	120		
50"	274	274	273	265	236	231	232		

Reactor Position (In.)	<u>0</u>	<u>2</u>	<u>4</u>	<u>6</u>	<u>8</u>	<u>10</u>	<u>12</u>	<u>14</u>	<u>16</u>	<u>18</u>
0	177	161	167	162	166	163	162	163	162	164
55	257	207	211	212	208	209	201	205	209	208
110	267	269	270	273	275	282	270	280	275	299
165	254	261	267	254	288	283	290	278	289	286
Min.	0	20	40	60	80	100	120			
55"	257	253	252	245	211	216	207			

EMB/ml
6/21/79

TABLE VI

EXPERIMENTAL TESTS COMPLETED

<u>Run No.</u>	<u>Catalyst</u>	<u>Liquid</u>	<u>Fines, Vol%</u>	<u>Test No.</u>	<u>Liquid Flow Rate, GPM/Ft²</u>	<u>Gas Flow Rate, Ft/Sec</u>
300	None	Kerosene	0.0	-01	22.4	0.05
				-02	22.3	0.10
				-03	22.3	0.15
				-04	22.4	0.20
				-05	22.4	0.25
				-06	44.9	0.05
				-07	44.6	0.10
				-08	44.9	0.15
				-09	44.5	0.20
				-10	45.2	0.23
				-11	66.6	0.05
				-12	66.9	0.10
				-13	67.3	0.15
				-14	66.6	0.21
				-15	66.7	0.25
				-16	88.7	0.05
				-17	88.8	0.11
				-18	89.7	0.16
				-19	89.8	0.23
				301	HDS-2A L = 3/8" D = 1/16"	Kerosene
-01	37.6	0.0				
-02	44.0	0.0				
-03	58.9	0.0				
-04	66.0	0.0				
-05	76.4	0.0				
-06	87.9	0.0				
-07	119.0	0.0				
-08	38.3	0.04				
-09	37.9	0.09				
-10	40.4	0.14				
-11	44.6	0.10				
-12	44.2	0.14				
-13	67.4	0.10				
-14	66.6	0.15				
-15	88.4	0.11				
-16	88.3	0.16				

TABLE VI
EXPERIMENTAL TESTS COMPLETED
-2-

Run No.	Catalyst	Cat. L/D	Liquid	Fines Vol %	Test No.	Liquid Flow Rate Gpm/Ft ²	Gas Flow Rate Ft/Sec
212	HDS-2A	3	Kerosene	0.0	- 1	30.8	0.0
	"	"	"	"	- 2	31.7	0.10
	"	"	"	"	- 3	45.0	0.0
	"	"	"	"	- 4	44.6	0.04
	"	"	"	"	- 5	44.0	0.10
	"	"	"	"	- 6	44.7	0.14
	"	"	"	"	- 7	66.8	0.0
	"	"	"	"	- 8	66.4	0.11
	"	"	"	"	- 9	66.5	0.16
	"	"	"	"	-10	88.7	0.0
	"	"	"	"	-11	88.4	0.12
	"	"	"	"	-12	45.2	0.19
	"	"	"	"	-13	66.5	0.21
	"	"	"	"	-14	88.3	0.23
	"	"	"	"	-15	87.8	0.16

TABLE VI

EXPERIMENTAL TESTS COMPLETED

-3-

Run No.	Catalyst	Cat. L/D	Liquid	Fines Vol %	Test No.	Liquid Flow Rate Gpm/Ft ²	Gas Flow Rate Ft/Sec
213	HDS-2A	3	Kerosene	0.0	- 1	38.4	0.0
	"	"	"	"	- 2	37.3	0.05
	"	"	"	"	- 3	37.4	0.10
	"	"	"	"	- 4	37.4	0.15
	"	"	"	"	- 5	44.3	0.05
	"	"	"	"	- 6	68.4	0.05
	"	"	"	"	- 7	89.1	0.05
	"	"	"	"	- 8	45.0	0.10
	"	"	"	"	- 9	36.7	0.20
	"	"	"	"	-10	44.4	0.20
	"	"	"	"	-11	66.4	0.20
	"	"	"	"	-12	37.5	0.25
	"	"	"	"	-13	44.0	0.25
	"	"	"	"	-14	66.5	0.25
	"	"	"	"	-15	88.1	0.25
	"	"	"	"	-16	88.4	0.20
	"	"	"	"	-17	88.7	0.10
	"	"	"	"	-18	87.2	0.15
	"	"	"	"	-19	44.4	0.15
	"	"	"	"	-20	66.6	0.15
	"	"	"	"	-21	66.7	0.10
	"	"	"	"	-22	109.5	0.05

TABLE VI
 EXPERIMENTAL TESTS COMPLETED
 -4-

Run No.	Catalyst	Cat. L/D	Liquid	Fines Vol %	Test No.	Liquid Flow Rate Gpm/Ft ²	Gas Flow Rate Ft/Sec
214	HDS-2A	3	KEROSENE	15.5	- 1	45.8	0.0
	"	"	"	"	- 2	43.4	0.0
	"	"	"	"	- 3	39.3	0.0
	"	"	"	"	- 4	31.2	0.0
	"	"	"	"	- 5	53.9	0.0
	"	"	"	"	- 6	60.3	0.0
	"	"	"	"	- 7	70.0	0.0
	"	"	"	"	- 8	71.4	0.0
	"	"	"	"	- 9	79.7	0.0

TABLE VII
CALCULATED HOLDUPS, RUN 300

<u>Run No.</u>	<u>$\epsilon_{1\gamma}$</u>	<u>$\epsilon_{1\Delta\phi}$</u>	<u>$\epsilon_{2\gamma}$</u>	<u>V_{CD} (mm/sec)</u>
300-01	0.95	0.96	0.05	13.7
-02	0.89	0.90	0.11	25.5
-03	0.86	0.85	0.14	37.2
-04	0.81	0.80	0.19	46.5
-05	0.78	0.79	0.22	56.1
-06	0.93	0.93	0.07	12.0
-07	0.84	0.86	0.16	30.8
-08	0.78	0.78	0.22	29.0
-09	0.69	0.73	0.31	31.7
-10	0.65	0.72	0.35	34.9
-11	0.90	0.94	0.10	9.1
-12	0.77	0.81	0.23	13.0
-13	0.71	0.75	0.29	19.2
-14	0.65	0.71	0.35	25.6
-15	0.64	0.69	0.36	32.3
-16	0.93	0.95	0.07	9.9
-17	0.83	0.85	0.17	17.5
-18	0.77	0.82	0.23	23.5
-19	0.71	0.74	0.29	31.2
-20	0.95	0.98	0.05	10.7

EMB/ml
 4/12/79

TABLE VIII

% BED EXPANSION FOR RUN 301: KEROSENE

<u>Run No.</u>	<u>Liquid Flow Rate, GPM/Ft²</u>	<u>Gas Flow Rate, Ft/Sec</u>	<u>Catalyst Bed Height, Inches</u>	<u>Bed Expansion, %</u>
Initial	--	--	43.9	-
301-01	37.6	0.0	47	7
-02	44.0	0.0	49	11
-03	58.9	0.0	51	16
-04	66.0	0.0	53	21
-05	76.4	0.0	55	25
-06	87.9	0.0	63	43
-07	119.0	0.0	97	121
-08	38.3	0.04	50	22
-09	37.9	0.09	51	24
-10	40.4	0.14	53	29
-11	44.6	0.10	54	32
-12	44.2	0.14	55	34
-13	67.4	0.10	67	63
-14	66.6	0.15	73	78
-15	88.4	0.11	83	102
-16	88.3	0.16	93	127

EMB/ml
4/12/79

TABLE IX

% BED EXPANSION FOR RUN 212

-33

CATALYST : HDS-2A
 LIQUID : KEROSENE
 COAL CHAR CONC: 0.0 VOL %
 TEMPERATURE : 71. DEG F

Run No.	Liquid Flow Rate, GPM/Ft ²	Gas Flow Rate Ft/Sec	Catalyst Bed Height (In.)	% Bed Expansion
212- 1	30.8	0.0	57.	14.
- 2	31.7	0.10	67.	34.
- 3	45.0	0.0	65.	30.
- 4	44.6	0.04	70.	40.
- 5	44.0	0.10	77.	54.
- 6	44.7	0.14	81.	62.
- 7	66.8	0.0	84.	68.
- 8	66.4	0.11	95.	90.
- 9	66.5	0.16	102.	104.
-10	88.7	0.0	109.	118.
-11	88.4	0.12	119.	138.
-12	45.2	0.19	82.	64.
-13	66.5	0.21	111.	122.
-14	88.3	0.23	134.	168.
-15	87.8	0.16	127.	154.

TABLE X

% BED EXPANSION FOR RUN 213

CATALYST : HDS-2A
 LIQUID : KEROSENE
 COAL CHAR CONC: 0.0 VOL %
 TEMPERATURE : 70. DEG F

Run No.	Liquid Flow Rate, GPM/Ft ²	Gas Flow Rate Ft/Sec	Catalyst Bed Height (In.)	% Bed Expansion
213- 1	38.4	0.0	63.	26.
- 2	37.3	0.05	64.	28.
- 3	37.4	0.10	68.	36.
- 4	37.4	0.15	71.	42.
- 5	44.3	0.05	69.	38.
- 6	68.4	0.05	86.	79.
- 7	89.1	0.05	109.	127.
- 8	45.0	0.10	70.	46.
- 9	36.7	0.20	69.	44.
-10	44.4	0.20	76.	58.
-11	66.4	0.20	93.	94.
-12	37.5	0.25	69.	44.
-13	44.0	0.25	75.	56.
-14	66.5	0.25	99.	106.
-15	88.1	0.25	125.	160.
-16	88.4	0.20	120.	150.
-17	88.7	0.10	111.	131.
-18	87.2	0.15	117.	144.
-19	44.4	0.15	76.	58.
-20	66.6	0.15	96.	100.
-21	66.7	0.10	91.	90.
-22	109.5	0.05	135.	181.

TABLE XI

% BED EXPANSION FOR RUN 214

CATALYST : HDS-2A
 LIQUID : KEROSENE
 COAL CHAR CONC: 15.5 VOL %
 TEMPERATURE : 150. DEG F

Run No.	Liquid Flow Rate, GPM/Ft ²	Gas Flow Rate Ft/Sec	Catalyst Bed Height (In.)	% Bed Expansion
214- 1	45.8	0.0	74.	40.
- 2	43.4	0.0	69.	30.
- 3	39.3	0.0	63.	19.
- 4	31.2	0.0	58.	9.
- 5	53.9	0.0	81.	53.
- 6	60.3	0.0	86.	62.
- 7	70.0	0.0	90.	70.
- 8	71.4	0.0	96.	81.
- 9	79.7	0.0	105.	98.

TABLE XII

CALCULATED HOLDUPS, RUN 301: DENSE PHASE

<u>Run No.</u>	<u>ϵ_c</u>	<u>$\epsilon_l \gamma$</u>	<u>$\epsilon_l \Delta P$</u>	<u>$\epsilon_{g\gamma}$</u>	<u>V_{CD} (mm/sec)</u>
301-01	0.42	0.64	0.73	0.0	--
-02	0.41	0.65	0.72	0.0	--
-03	0.39	0.66	0.72	0.0	--
-04	0.38	0.67	0.71	0.0	--
-05	0.36	0.68	0.70	0.0	--
-06	0.32	0.72	0.70	0.0	--
-07	0.21	0.82	0.78	0.0	--
-08	0.37	0.50	0.46	0.12	5.4
-09	0.36	0.51	0.41	0.12	18.8
-10	0.35	0.52	0.41	0.13	31.2
-11	0.34	0.60	0.45	0.06	25.8
-12	0.34	0.58	0.42	0.08	35.4
-13	0.28	0.63	0.58	0.09	21.8
-14	0.25	0.53	0.57	0.21	21.8
-15	0.22	0.61	0.67	0.17	13.7
-16	0.20	0.58	0.65	0.22	20.0

EMB/ml
4/12/79

TABLE XIII
CALCULATED HOLDUPS, RUN 212: DENSE PHASE

-37

CATALYST : HDS-2A
LIQUID : KEROSENE
COAL CHAR CONC: 0.0 VOL %
TEMPERATURE : 71. DEG F

Run No.	Liquid Flow Rate, Gpm/Ft ²	Gas Flow Rate, Ft/Sec	ϵ_c	ϵ_{ly}	ϵ_{LAP}	ϵ_{gz}	Vcd (Mm/Sec)
212- 1	30.8	0.0	0.43	0.64	0.63	0.0	0.0
- 2	31.7	0.10	0.37	0.46	0.46	0.18	17.7
- 3	45.0	0.0	0.38	0.71	0.64	0.0	0.0
- 4	44.6	0.04	0.35	0.49	0.55	0.16	3.1
- 5	44.0	0.10	0.32	0.42	0.50	0.26	9.1
- 6	44.7	0.14	0.30	0.40	0.47	0.30	15.0
- 7	66.8	0.0	0.29	0.76	0.72	0.0	0.0
- 8	66.4	0.11	0.26	0.52	0.58	0.23	10.7
- 9	66.5	0.16	0.24	0.48	0.54	0.28	15.8
-10	88.7	0.0	0.22	0.82	0.77	0.0	0.0
-11	88.4	0.12	0.21	0.60	0.65	0.19	13.8
-12	45.2	0.19	0.30	0.36	0.45	0.34	19.5
-13	66.5	0.21	0.22	0.46	0.53	0.32	22.6
-14	88.3	0.23	0.18	0.51	0.58	0.31	23.7
-15	87.8	0.16	0.19	0.59	0.64	0.22	21.3

TABLE XIV

CALCULATED HOLDUPS, RUN 213: DENSE PHASE

-38

CATALYST : HDS-2A
 LIQUID : KEROSENE
 COAL CHAR CONC: 0.0 VOL %
 TEMPERATURE : 70. DEG F

Run No.	Liquid Flow Rate, Gpm/Ft ²	Gas Flow Rate, Ft/Sec					ϵ_{gY}	Vcd (Mm/Sec)
		ϵ_c	ϵ_{LY}	ϵ_{LAP}	ϵ_{gY}			
213- 1	38.4	0.0	0.39	0.68	0.62	0.0	0.0	
- 2	37.3	0.05	0.38	0.48	0.55	0.14	6.6	
- 3	37.4	0.10	0.36	0.45	0.53	0.19	16.0	
- 4	37.4	0.15	0.35	0.41	0.50	0.24	23.5	
- 5	44.3	0.05	0.36	0.49	0.58	0.15	5.2	
- 6	68.4	0.05	0.27	0.64	0.68	0.09	8.1	
- 7	89.1	0.05	0.22	0.71	0.76	0.07	8.2	
- 8	45.0	0.10	0.34	0.51	0.56	0.15	18.4	
- 9	36.7	0.20	0.34	0.51	0.54	0.15	45.2	
-10	44.4	0.20	0.31	0.52	0.56	0.17	42.4	
-11	66.4	0.20	0.25	0.55	0.62	0.20	36.1	
-12	37.5	0.25	0.34	0.44	0.52	0.22	50.1	
-13	44.0	0.25	0.31	0.42	0.53	0.27	42.0	
-14	66.5	0.25	0.24	0.55	0.60	0.21	46.8	
-15	88.1	0.25	0.19	0.59	0.66	0.22	42.5	
-16	88.4	0.20	0.20	0.61	0.67	0.20	33.4	
-17	88.7	0.10	0.21	0.66	0.73	0.13	16.7	
-18	87.2	0.15	0.20	0.63	0.68	0.17	25.0	
-19	44.4	0.15	0.31	0.51	0.55	0.18	28.4	
-20	66.6	0.15	0.24	0.56	0.61	0.20	23.6	
-21	66.7	0.10	0.26	0.57	0.64	0.17	14.3	
-22	109.5	0.05	0.17	0.76	0.80	0.07	8.3	

TABLE XV

CALCULATED HOLDUPS, RUN 214: DENSE PHASE

CATALYST : HDS-2A
 LIQUID : KEROSENE
 COAL CHAR CONC: 15.5 VOL %
 TEMPERATURE : 150. DEG F

Run No.	Liquid Flow Rate, Gpa/Ft ²	Gas Flow Rate, Ft/Sec	ϵ_c	$\epsilon_{1\gamma}$	$\epsilon_{1\Delta P}$	ϵ_g	U_{cd} (Ma/Sec)
214- 1	45.8	0.0	0.35	0.65	0.63	0.0	0.0
- 2	43.4	0.0	0.38	0.66	0.62	0.0	0.0
- 3	39.3	0.0	0.41	0.63	0.59	0.0	0.0
- 4	31.2	0.0	0.45	0.60	0.59	0.0	0.0
- 5	53.9	0.0	0.32	0.68	0.64	0.0	0.0
- 6	60.3	0.0	0.30	0.69	0.65	0.0	0.0
- 7	70.0	0.0	0.29	0.70	0.66	0.0	0.0
- 8	71.4	0.0	0.27	0.71	0.68	0.0	0.0
- 9	79.7	0.0	0.25	0.71	0.69	0.0	0.0

TABLE XVI

CALCULATED HOLDUPS, RUN 301: DILUTE PHASE

<u>Run No.</u>	<u>ϵ_{1Y}</u>	<u>ϵ_{1AP}</u>	<u>ϵ_{gY}</u>
301-01	0.98	0.97	0.0
-02	0.98	0.98	0.0
-03	0.98	0.98	0.0
-04	0.99	0.97	0.0
-05	0.99	0.97	0.0
-06	0.99	0.97	0.0
-07	0.99	0.96	0.0
-08	0.86	0.93	0.14
-09	0.74	0.81	0.26
-10	0.67	0.76	0.33
-11	0.72	0.80	0.28
-12	0.64	0.72	0.36
-13	0.73	0.80	0.27
-14	0.69	0.76	0.31
-15	0.79	0.86	0.21
-16	0.72	0.81	0.28

EMB/ml
4/12/79

TABLE XVII

CALCULATED HOLDUPS, RUN 212--DILUTE PHASE

CATALYST : HDS-2A
 LIQUID : KEROSENE
 COAL CHAR CONC: 0.0 VOL %
 TEMPERATURE : 71. DEG F

Run No.	Liquid Flow Rate, Gpm/Ft ²	Gas Flow Rate, Ft/Sec	ϵ_{1Y}	ϵ_{1AP}	ϵ_{2Y}
212- 1	30.8	0.0	0.98	0.94	0.0
- 2	31.7	0.10	0.76	0.87	0.24
- 3	45.0	0.0	0.98	0.94	0.0
- 4	44.6	0.04	0.86	0.96	0.14
- 5	44.0	0.10	0.74	0.85	0.26
- 6	44.7	0.14	0.65	0.78	0.35
- 7	66.8	0.0	0.98	0.94	0.0
- 8	66.4	0.11	0.75	0.86	0.25
- 9	66.5	0.16	0.68	0.79	0.32
-10	88.7	0.0	0.98	0.94	0.0
-11	88.4	0.12	0.77	0.88	0.23
-12	45.2	0.19	0.64	0.76	0.36
-13	66.5	0.21	0.61	0.73	0.39
-14	88.3	0.23	0.64	0.80	0.36
-15	87.8	0.16	0.72	0.83	0.28

TABLE XVIII
CALCULATED HOLDUPS, RUN 213--DILUTE PHASE -42

CATALYST : HDS-2A
LIQUID : KEROSENE
COAL CHAR CONC: 0.0 VOL %
TEMPERATURE : 70. DEG F

Run No.	Liquid Flow Rate, Gpm/Ft ²	Gas Flow Rate, Ft/Sec	ϵ_{1Y}	ϵ_{1AP}	ϵ_{gY}
213- 1	38.4	0.0	0.98	0.94	0.0
- 2	37.3	0.05	0.92	1.01	0.08
- 3	37.4	0.10	0.85	0.95	0.15
- 4	37.4	0.15	0.78	0.89	0.22
- 5	44.3	0.05	0.89	0.99	0.11
- 6	68.4	0.05	0.92	0.98	0.08
- 7	89.1	0.05	0.90	1.03	0.10
- 8	45.0	0.10	0.87	0.93	0.13
- 9	36.7	0.20	0.78	0.93	0.22
-10	44.4	0.20	0.75	0.91	0.25
-11	66.4	0.20	0.74	0.89	0.26
-12	37.5	0.25	0.75	0.91	0.25
-13	44.0	0.25	0.73	0.89	0.27
-14	66.5	0.25	0.69	0.85	0.31
-15	88.1	0.25	0.70	0.86	0.30
-16	88.4	0.20	0.73	0.89	0.27
-17	88.7	0.10	0.83	0.98	0.17
-18	87.2	0.15	0.76	0.91	0.24
-19	44.4	0.15	0.75	0.90	0.25
-20	66.6	0.15	0.74	0.89	0.26
-21	66.7	0.10	0.80	0.95	0.20
-22	109.5	0.05	0.89	1.07	0.11

TABLE XIX

*43

BHATTIA-EPSTEIN MODEL RESULTS: RUN 212
Kerosene/0% Fines/Nitrogen

	U_l	U_g	X_k	U_{cb}	ϵ_c	ϵ_{c_c}	ϵ_l	ϵ_{l_c}	ϵ_g	ϵ_{g_c}
	ft/sec		ft/sec							
212-01	.07	0	-	-	0.43	-	0.62	-	0.0	-
-02	.07	0.1	-	-	0.37	-	0.46	-	0.17	-
-03	0.10	0	-	-	0.38	-	0.71	-	0	-
-04	0.10	0.04	0.0	0.001	0.35	0.33	0.49	0.52	0.16	0.15
-05	0.10	0.10	0.0	0.01	0.32	0.29	0.42	0.47	0.26	0.26
-06	0.10	0.14	0.0	0.03	0.30	0.27	0.40	0.43	0.30	0.3
-07	0.15	0	-	-	0.29	-	0.76	-	0	-
-08	0.15	0.11	0.0	0.02	0.25	0.23	0.52	0.54	0.23	0.23
-09	0.15	0.15	0.0	0.01	0.24	0.21	0.48	0.51	0.28	0.28
-10	0.2	0	-	-	0.22	-	0.82	-	0	-
-11	0.2	0.12	0.02	0.12	0.21	0.2	0.60	0.61	0.19	0.19
-12	0.1	0.2	0.22	0.05	0.30	0.26	0.36	0.40	0.34	0.34
-13	0.15	0.21	0.13	0.05	0.22	0.21	0.46	0.48	0.32	0.32
-14	0.2	0.23	0.02	0.03	0.18	0.17	0.51	0.52	0.31	0.31
-15	0.2	0.16	0.23	0.1	0.19	0.18	0.59	0.59	0.22	0.23

$\epsilon_c, \epsilon_l, \epsilon_g$ - Experimental Holdups

$\epsilon_{c_c}, \epsilon_{l_c}, \epsilon_{g_c}$ - Holdups calculated by Bhatia-Epstein Model

TABLE XX

BHATIA-EPSTEIN MODEL RESULTS: RUN 213
Kerosene/0% Fines/Helium

	U_l	U_g	X_k	U_{t_b}	ϵ_c	ϵ_{c_c}	ϵ_l	ϵ_{l_c}	ϵ_g	ϵ_{g_c}
	ft/sec		ft/sec							
213-01	0.085	2.0	0	-	0.39	-	0.68	-	0.0	-
-02	0.083	0.05	0.14	0.08	0.38	0.37	0.48	0.48	0.14	0.15
-03	0.083	0.10	0.52	0.17	0.36	0.34	0.45	0.46	0.19	0.19
-04	0.083	0.15	0.59	0.2	0.35	0.32	0.41	0.44	0.24	0.24
-05	0.10	0.05	0.0	0.06	0.36	0.34	0.49	0.52	0.15	0.15
-06	0.15	0.05	0.36	0.24	0.27	0.3	0.64	0.61	0.09	0.09
-07	0.20	0.05	0.77	0.4	0.22	0.24	0.71	0.70	0.07	0.07
-08	0.10	0.10	0.64	0.3	0.34	0.34	0.51	0.51	0.15	0.15
-09	0.082	0.20	0.87	0.8	0.34	0.37	0.51	0.48	0.15	0.15
-10	0.10	0.20	0.83	0.6	0.31	0.32	0.52	0.50	0.17	0.18
-11	0.15	0.20	0.68	0.45	0.25	0.25	0.55	0.56	0.20	0.19
-12	0.085	0.25	0.83	0.55	0.34	0.33	0.44	0.46	0.22	0.22
-13	0.10	0.25	0.72	0.35	0.31	0.28	0.42	0.46	0.27	0.26
-14	0.15	0.25	0.78	0.55	0.24	0.23	0.55	0.56	0.21	0.21
-15	0.20	0.25	0.65	0.45	0.19	0.18	0.59	0.60	0.22	0.22
-16	0.20	0.20	0.60	0.35	0.20	0.18	0.61	0.61	0.20	0.2
-17	0.20	0.10	0.47	0.3	0.21	0.22	0.66	0.65	0.13	0.13
-18	0.20	0.15	0.56	0.35	0.20	0.20	0.63	0.63	0.17	0.17
-19	0.10	0.15	0.73	0.4	0.31	0.32	0.51	0.50	0.18	0.18
-20	0.15	0.15	0.51	0.25	0.24	0.24	0.56	0.56	0.20	0.20
-21	0.15	0.10	0.33	0.15	0.26	0.25	0.57	0.57	0.17	0.17
-22	0.24	0.05	0.38	0.25	0.17	0.20	0.76	0.73	0.07	0.07

$\epsilon_c, \epsilon_l, \epsilon_g$ - Experimental Holdups

$\epsilon_{c_c}, \epsilon_{l_c}, \epsilon_{g_c}$ - Holdups Calculated by Bhatia-Epstein Model

TABLE XXI

BHATIA-EPSTEIN MODEL RESULTS: RUN 100--
WATER/O% FINES/NITROGEN

<u>Test No.</u>	<u>U₁</u> <u>Ft/Sec</u>	<u>U_g</u> <u>Ft/Sec</u>	<u>X_t</u> <u>Ft/Sec</u>	<u>U_{t₃}</u> <u>Ft/Sec</u>	<u>ε_c</u>	<u>ε_{c_c}</u>	<u>ε₁</u>	<u>ε_{1_c}</u>	<u>ε_g</u>	<u>ε_{g_c}</u>
100-09	0.1	0.05	0.80	0.7	0.41	0.42	0.54	0.53	0.05	0.05
-10	0.1	0.10	0.87	1.0	0.40	0.40	0.53	0.52	0.07	0.07
-11	0.1	0.15	0.95	2.5	0.39	0.42	0.56	0.53	0.05	0.05
-12	0.1	0.20	0.96	3.3	0.37	0.42	0.58	0.53	0.05	0.05
-13	0.15	0.05	0.43	0.3	0.31	0.31	0.61	0.61	0.08	0.08
-14	0.15	0.10	0.75	0.7	0.30	0.30	0.61	0.61	0.09	0.09
-15	0.15	0.15	0.82	1.0	0.31	0.29	0.59	0.61	0.10	0.10
-16	0.15	0.20	0.87	1.4	0.31	0.29	0.59	0.61	0.10	0.10
-17	0.2	0.05	0.65	0.7	0.25	0.25	0.70	0.71	0.05	0.05
-18	0.2	0.10	0.67	1.0	0.25	0.22	0.66	0.69	0.09	0.09

EMB/ml
6/21/79

TABLE XXII

BHATIA EPSTEIN MODEL RESULTS: RUN 206 58-74 (211)--
 KEROSENE/16.5 VOL% FINES/NITROGEN

<u>Test No.</u>	<u>$\frac{U_1}{\text{Ft/Sec}}$</u>	<u>$\frac{U_g}{\text{Ft/Sec}}$</u>	<u>$\frac{X_{Kc}}{\text{Ft/Sec}}$</u>	<u>$\frac{U_{T_B}}{\text{Ft/Sec}}$</u>	<u>ϵ_c</u>	<u>ϵ_{c_c}</u>	<u>ϵ_{s1}</u>	<u>ϵ_{s1_c}</u>	<u>ϵ_g</u>	<u>ϵ_{g_c}</u>
206-58	0.085	0.05	0.82	0.56	0.34	0.33	0.60	0.61	0.06	0.06
-59	"	0.10	0.89	1.0	0.32	0.32	0.60	0.60	0.08	0.08
-60	"	0.15	0.93	1.5	0.30	0.32	0.60	0.60	0.08	0.08
-61	"	0.20	0.94	2.0	0.29	0.32	0.63	0.60	0.08	0.08
-62	"	0.25	0.95	2.2	0.29	0.31	0.62	0.60	0.09	0.09
-64	0.10	0.05	0.84	0.6	0.29	0.30	0.66	0.64	0.05	0.06
-65	"	0.10	0.80	0.56	0.29	0.28	0.60	0.61	0.11	0.11
-66	"	0.15	0.89	1.0	0.29	0.28	0.61	0.61	0.10	0.11
-67	"	0.20	0.93	1.5	0.27	0.28	0.64	0.62	0.09	0.10
-68	"	0.25	0.95	2.4	0.27	0.29	0.64	0.62	0.09	0.09
-70	0.15	0.05	0.77	0.56	0.22	0.23	0.73	0.71	0.05	0.06
-71	"	0.10	0.64	0.45	0.20	0.21	0.67	0.67	0.13	0.12
-72	"	0.15	0.78	0.7	0.23	0.21	0.64	0.66	0.13	0.13
-73	"	0.20	0.82	0.9	0.23	0.2	0.63	0.66	0.14	0.14
-74	"	0.25	0.85	1.0	0.23	0.2	0.62	0.65	0.15	0.16

EMB/ml
 6/21/79

TABLE XXIII

CONDITIONS OF TRACER TESTS PERFORMED 4/6/79:
KEROSENE, NITROGEN, 70°F

<u>Test No.</u>	<u>U₁ Ft/Sec</u>	<u>U_g Ft/Sec</u>	
1	0.10	0.10	
2	"	"	
3	"	"	
4	"	"	
5	"	"	
6	"	"	
7	"	"	
8	"	"	
9	"	"	
10	"	"	
11	"	"	} View on Detector 3 reduced from entire reactor to only reactor center.
12	"	"	
13	"	"	
14	"	0.05	} View on Detector 3 opened again.
15	"	"	
16	"	0.20	
17	"	"	

EMB/ml
5/16/79

TABLE XXIV

CONDITIONS OF TRACER TESTS PERFORMED 4/20/79:
KEROSENE, NITROGEN, HDS-2A 1 = 3/16" CATALYST, 70°F

<u>Test No.</u>	<u>U₁ Ft/Sec</u>	<u>U_g Ft/Sec</u>	<u>Injection</u>
1	0.10	0.10	Spool Piece
2	"	"	"
3	"	"	"
4	"	"	"
5	"	"	"
6	"	"	"
7	"	"	"
8	"	"	"
9	"	"	"
10	"	"	"
11	"	0.05	"
12	"	"	"
13	"	0.20	"
14	"	"	"
15	"	0.10	Upstream of Bubble Cup
16	"	"	"

EMB/ml
5/16/79

TABLE XXV

CONDITIONS OF TRACER TEST PERFORMED 5/15/79:
KEROSENE/15 VOL% COAL CHAR/NITROGEN/HDS-2A 1/d = 3, 70°F

<u>Test No.</u>	<u>U₁</u> <u>Ft/Sec</u>	<u>Ft/Sec</u>	<u>Injection</u>
1	0.10	0.10	Spool Piece
2	0.10	0.10	"
3	0.10	0.10	"
4	0.10	0.10	"
5	0.10	0.10	"
6	0.10	0.10	"
7	0.10	0.10	"
8	0.10	0.10	"
9	0.10	0.10	"
10	0.10	0.10	"
11	0.10	0.05	"
12	0.10	0.05	"
13	0.10	0.05	"
14	0.10	0.15	"
15	0.10	0.15	"
16	0.10	0.10	Bubble Cap
17	0.085	0.20	Spool Piece
18	0.085	0.20	"

EMB/ml
6/21/79